Chapter 17
Flagellated Bacterial Nanorobots for Medical Interventions in the Human Body

Sylvain Martel

Abstract Enhancing targeting in the smallest blood vessels found in the human microvasculature will most likely require the use of various types of microdevices and nanorobots. As such, biology may play an important role where medical bio-nanorobots including nanorobots propelled in the microvasculature by flagellated bacteria to target deep regions in the human body will become important candidates for such applications. In this chapter, we introduce the concept and show the advantages of integrating biological components and more specifically Magneto-tactic Bacteria (MTB) for the development of hybrid nanorobots, i.e., nanorobots made of synthetic and biological nanoscale components, designed to operate efficiently in the human microvascular network. Similarly, the chapter shows the advantage of using Magnetic Resonance Imaging (MRI) as an imaging modality to control and track such medical nanorobots when operating inside the complex human vascular network. The chapter also presents preliminary experimental results suggesting the feasibility of guiding and controlling these nanorobots directly towards specific locations deep inside the human body.

Keywords Bacteria · Nanorobots · Magnetic Resonance Imaging (MRI) · Medical interventions · Tumor targeting

17.1 Introduction and Motivation

Nanorobots capable of operating inside the human body could potentially help various medical cases including but not limited to tumor targeting, arteriosclerosis,

S. Martel (✉)
NanoRobotics Laboratory, Department of Computer and Software Engineering,
Institute of Biomedical Engineering École Polytechnique, de Montréal (EPM),
Station Centre-Ville, Montréal, QC, Canada
e-mail: sylvain.martel@polymtl.ca

J. Rosen et al. (eds.), *Surgical Robotics: Systems Applications and Visions*,
DOI 10.1007/978-1-4419-1126-1_17,

blood clots leading to stroke, accumulation of scar tissue, localized pockets of infection, and many more.

While much speculation has been published on possible far-future applications of nanorobots, i.e., miniature robots based on nanotechnology using advanced materials and manufacturing techniques, little has been published on applying existing engineering technology with biology to implement systems beyond traditional technological limitations allowing such devices to operate in the human vascular network.

There exist several definitions of nanorobots describing different types, from relatively large robotic platform capable of operations at the nanoscale, to the theoretical version of robots with overall dimensions in the nanometer-scale. Theoretical indeed since the implementation of true robots and especially medical robots with overall dimensions of less than approximately 100 nm (being considered as the upper limit in nanotechnology), is well beyond today's technology. Therefore, a new definition for nanorobots that reflects more the reality of what can be achieved has recently emerged, defining such nanorobots has robots with overall dimensions in the micrometer-scale that rely on nanoscale components to enable us to embed particular functionalities. Similarly, medical nanorobots are defined here as microscale robots that exploit nanometer-scale components and phenomena while applying principles of robotics combined with nanomedicine to provide new medical diagnostic and interventional tools. Although there are many potential applications that could take advantage of such nanorobots, tumor targeting for therapeutic purpose has been chosen in this chapter as an important yet challenging application in medicine where such nanorobots could bring significant outcomes.

17.1.1 Main Accessible Regions for Untethered Robots in the Human Body

There are many regions in the human body which can be accessible for untethered robots. Many of these regions can be classified as direct line-of-sight regions, meaning that many visualization and/or tracking techniques (with or without microscopy) used in traditional robotics can feed back information to a controller for servo-control of the untethered robot. This is important since the imaging modality being used may impact and often complicate the control loop implementation by adding significant latencies that would prevent achieving control stability. Some of these regions that could be classified as direct line-of-sight include areas such as inside the mouth, the ears, or the eyes.

Other regions in the human body where direct line-of-sight is not possible include regions such as the digestive track and the vascular network, to name but only two main regions where significant research efforts are underway. In regions such as the digestive track, larger sized robots are more appropriate than microscale robots whereas in the human vasculature, microscale untethered robots become

more appropriate. In general, the human vascular network offer more potential for interventions, especially when we consider that it offers close to 100,000 km of routes to access the various regions inside the human body.

The diameter of the various blood vessels in the human vasculature dictates the overall dimensions of the untethered robots. In larger blood vessels such as the arteries, the maximum diameter is a few millimeters. The carotid artery for instance has a diameter of approximately 4–5 mm. Because of the various factors including wall effects which would add drag force to the robots, the diameter of a single robot navigating in such vessels should be approximately no more than half the diameter of the vessels being traveled.

To reach the capillary networks, such robots must travel through the arterioles. Since the diameters of the arterioles may vary from approximately 150 μm down to approximately 50 μm, an overall diameter for each robot of no more than approximately 25 μm would be necessary to reach the capillaries. To reach a target such as a tumor, each robot would have to travel through the capillaries. These capillaries may have a diameter as small as approximately 4 μm, meaning that the maximum diameter of an untethered robot designed to target a tumor should not be larger than approximately 2 μm. Interesting enough is the fact that the same robot does not need to be smaller than 2 μm in diameter unless it must go through the Blood Brain Barrier (BBB).

17.1.2 Embedded Synthetic Versus Biological Propulsion System

Tumoral lesions can be accessed by transiting through anarchic arteriocapillar networks stimulated by tumoral angiogenesis where capillaries located near the tumor could have diameters as small as a red blood cell. Hence, it becomes obvious that the development of self-propelled medical nanorobots relying on an embedded source of propulsion based on a synthetic machine such as envisioned in [1] for instance and capable of providing sufficient thrust force to operate in the human microvasculature, cannot be implemented considering actual technological advances.

As such, existing biological motors such as the molecular motors of bacteria with the attached flagella acting like propellers, becomes an interesting option for nanorobots, especially medical nanorobots operating in the bloodstreams [2, 3]. The flagellated bacteria of type MC-1 for instance is at this time considered to be one of the best candidates for such application for several reasons. First, the diameter of the MC-1 bacterium is ~2 μm being approximately half the diameter of the smallest capillaries found in human. Second, initial tests performed in mice have demonstrated potential for biocompatibility with proper initial response of the immune system. Third, experiments already showed that each bacterium provides thrust force exceeding 4 pico-Newtons (pN) which is at least ten times the thrust force provided by most species of flagellated bacteria. Hence, knowing present technological limits, such flagellated bacterium can be considered as a serious bio-actuator for nanorobots designed to operate in the microvasculature.

17.1.3 Directional Control

Although propulsion is an important factor, directional control is a must when nanorobots must be navigated in complex vascular networks. In [4], the first random motion of an auto-mobile microchip with flagellated bacteria attached was observed. But for targeting specific regions in the human body as in most other applications that could be envisioned with micro-nanorobots propelled by bacteria, steering or displacement control becomes essential. Some level of control of flagellated bacteria has been demonstrated such as chemical stop/resume [5] and phototaxis stop/resume [6] controls. But so far, only a directional control method based on magnetotaxis seems to be suitable for operations in the microvasculature. Although accurate chemotaxis-based steering control performed by computer has not been demonstrated yet, the use of chemicals may in a practical point of view, be extremely difficult if feasible to apply in the human microvasculature. Similarly, phototaxis-based directional control may not be applicable especially when targeting deep in the human body.

But accurate steering control deep in the human body can be achieved with the use of flagellated Magnetotactic Bacteria (MTB). Already, computer steering or control along a pre-programmed path [7] of a flagellated MTB has been demonstrated [8].

Magnetotaxis-based directional control induces a directional torque to a chain of membrane-based nanoparticles (referred to as magnetosomes) embedded in the cell of the MTB. The torque is induced from electrical currents flowing in a special conductor network surrounding the patient. When interfaced to a computer, automatic directional control can be achieved [8].

17.2 Bacterial Mechanical Power, Propulsion, Steering and Tracking

The four fundamental functions that must be embedded in an untethered microscale nanorobot designed to travel in the human microvascular networks are the mechanical power source, the propulsion system, the steering system, and some sort of beacons allowing such nanorobots to be tracked inside the human body.

Interesting enough is the fact all these four fundamental requirements are already embedded in each MC-1 bacterium as depicted in Fig. 17.1.

As depicted in Fig. 17.1, the diameter of the MC-1 magnetotactic bacterium which is spherical in shape, has a diameter of approximately 2 μm, allowing it to operate in the smallest diameter blood vessels found in human.

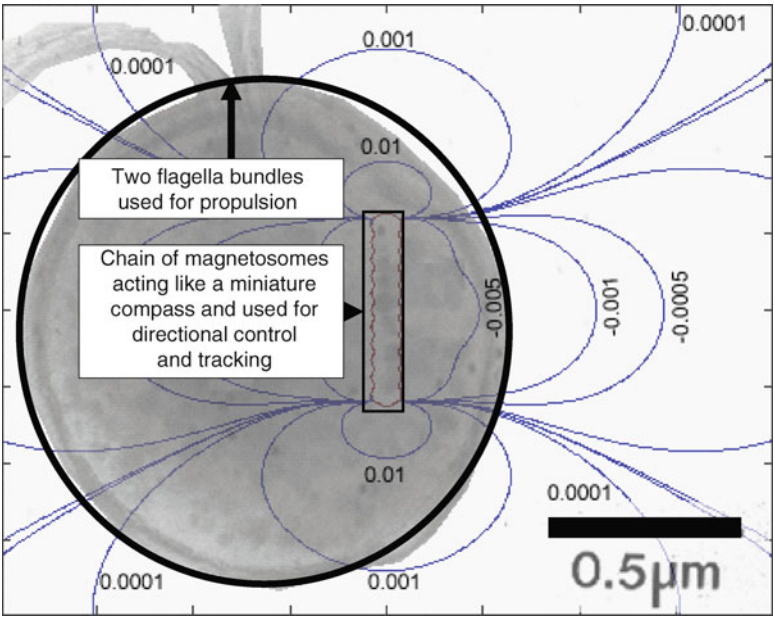

Fig. 17.1 A single MC-1 magnetotactic bacterium imaged using an electron microscope. Propulsion is provided by two flagella bundles while a chain of magnetosomes is used for directional control and tracking. The lines superposed over the image indicate the magnitude of distortion created by the magnetosomes when placed inside an MRI system allowing the bacteria to be tracked deep in the human vasculature where direct line-of-sight is not possible

17.2.1 Bacterial Mechanical Power

The use of bacteria by itself resolves one of the biggest challenges in artificially made micro- or nanorobots since no appropriate technology is available to embed sufficient power within such space constraints. Especially with a microscale robot with overall dimensions of only 2 μm across, the only alternative for engineers and researchers is to induce the power from an external source. An obvious solution which was and remains the most popular to date, is to induce a mechanical force using an external magnetic field typically generated from coils surrounding the patient or the part of the body where the intervention is being performed. Nonetheless, this solution has limitation especially when the distance from the coils and the microscale robots increase to accommodate operation deep in the human body, especially when operating deep in the human torso. In the latter case for instance, overheating of the coils would most likely prevent their usage for such applications. Therefore, an embedded source of propulsion would become more appropriate.

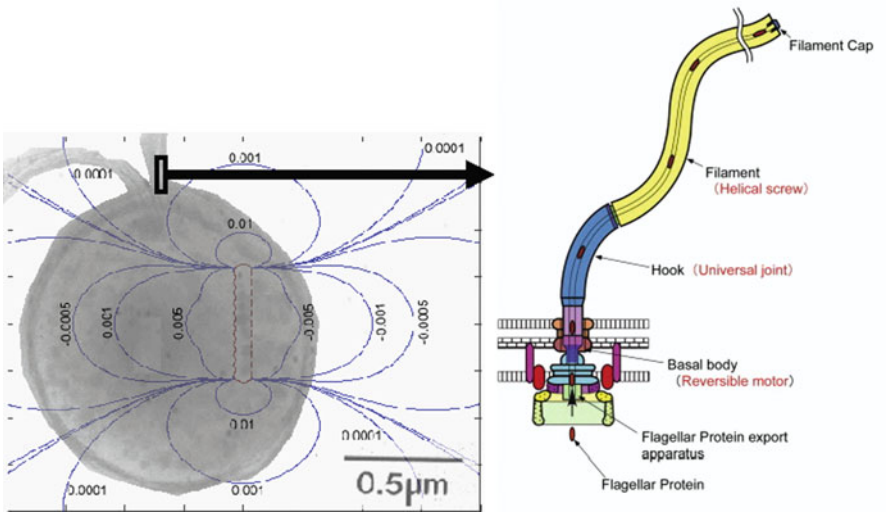

Fig. 17.2 Schematic diagrams of the flagellum connected to the molecular motor of a bacterium. As shown in the figure, the design of this molecular motor is very similar to an artificial version with a rotor inside a stator separated by ball-bearings. This molecular structure consists of three main parts: the basal body, which acts as a reversible rotary motor; the hook, which functions as a universal joint; and the filament, which acts as a helical screw (*OM*: Outer Membrane; PG: Peptidoglycan layer; CM: Cytoplasmic Membrane. (Adapted from Fig. 17.1 in Minamino T. et al. Molecular motors of the bacterial flagella. Curr. Opin. Struct. Biol. **18**, 693–701 (2008))

17.2.2 Bacterial Propulsion System

Each flagellum acting as a propeller is connected to a hook acting as a universal joint that connects to a molecular motor as depicted in Fig. 17.2. The MC-1 bacterium has two bundles of such flagella providing a total thrust force for propulsion between 4.0–4.7 pN $>$ 0.3–0.5 pN for many flagellated bacteria. Each flagellum rotates 360 degrees like a shaft in standard motor and can be reversed for backward motion. The total diameter of each molecular motor is less than 300 nm.

The flagellum acting like a propeller consists of a 20 nm-thick hollow tube. As depicted in the figure, the flagellum next to the outer membrane of the cell has a helical shape with a sharp bend outside. Together, this structure appears like a hook with a shaft running between the hook and the basal body. Similar to the architecture of a potential future artificial version, the shaft then passes through protein rings that act as bearings. For this nanometer-scale propulsion system, counterclockwise rotations of a polar flagellum will thrust the cell forward while clockwise rotations will result in the cell or the microstructure attached to, to move backward.

Experiments conducted in water and in human blood showed an average velocity for the MC-1 bacteria often exceeding 200 μm/s (compared to an average

velocity of approximately 30 μm/s for many other flagellated bacteria). Peak velocities of approximately 300 μm/s, i.e., 150 times its own cell's length per second have also been recorded.

17.2.3 Bacterial Steering System

The direction of motion of most flagellated bacteria is mainly influenced by chemotaxis. With chemotaxis, the swimming direction and the motility of bacteria is influenced by chemical gradients such as nutrient gradients [9–11]. Hence, a chemical approach would first appear to be the appropriate strategy to be used for the directional control of most flagellated bacteria. But although a chemical approach could be suitable in many applications, chemotaxis-based directional control in the human vasculature may be very difficult if suitable to be considered. Furthermore, chemotaxis-based directional control if feasible in the human body may not provide an adequate interface with computers or electronic controllers, which may be an essential requirement for a robotic platform where automatic and accurate motion control along pre-planned paths in the blood vessels must be implemented.

On the other hand, with the right species of flagellated bacteria, such as MTB, a low intensity directional electro-magnetic field capable of penetrating the human body with ease and without harm for the patient can be used while being compatible and easily interfaced with electronic computers and controllers.

For MTB, each cell (body) contains a naturally growth chain of magnetosomes which are membrane-based nanoparticles of a magnetic iron, e.g., iron-oxide for the MC-1 cells. Each nanoparticle has a diameter of only a few tens of nanometers and therefore will show single magnetic domain behavior. This chain acts like a nanometer-sized compass needle and will be oriented with the lines of magnetic field towards an artificial pole generated by computer.

The motion behavior of the MC-1 bacteria can be influenced in many ways including chemotaxis, phototaxis, aerotaxis, and magnetotaxis [12–14], the latter being more appropriate for automatic closed-loop navigation control in the vascular system.

To achieve better computerized control on the swimming direction of the MC-1 cells, the modes which are not or cannot be under the influence of an electronic controller or a software program and which would add uncertainties and errors along a pre-defined swimming path through unpredicted motion behaviors must become negligible. To achieve this, a very low intensity directional magnetic field but slightly higher than the Earth's geomagnetic field of 0.5 G is then applied. When doing so, the directional motion of these self-propelled bacterial steering systems become mainly influenced by magnetotaxis and therefore fully controllable as demonstrated in [8] (Fig. 17.3).

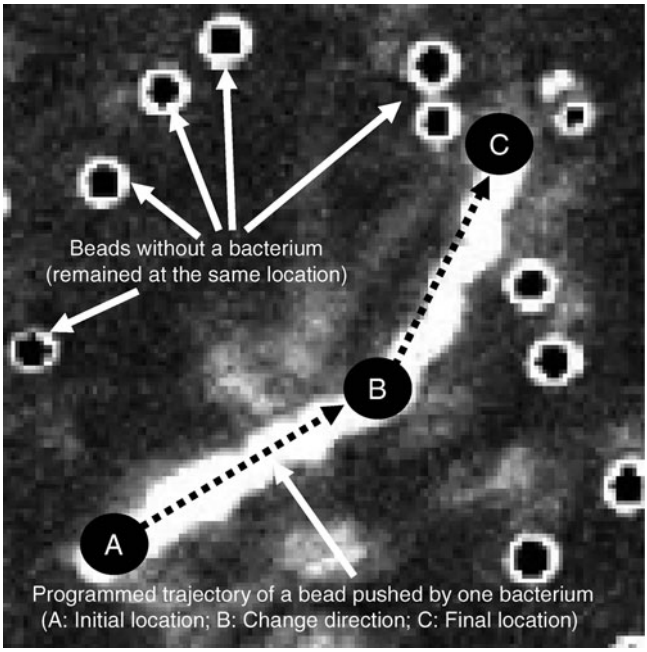

Fig. 17.3 These experimental results captured with an optical microscope, validate the concept of using a single flagellated magnetotactic bacterium as a self-propelled steering system for a microscale robot. Here a single flagellated bacterium was attached using specific antibodies to a 3-μm bead representing the artificial structure or body of a hybrid microrobot. As shown in the upper left section of the image, one can see that such microrobot represented by the bead can be pushed efficiently by a single flagellated bacterium. The lower left section shows the same bead represented by the black circles with numbers along a pre-programmed trajectory and corresponding to a sequence of software instructions, proving that accurate computer-based control of a bacterial propulsion and steering system is possible

17.2.4 Bacterial Tracking System

It does not matter how smart is a nanorobot, for targeting a specific region such as a tumor, any nanorobots will get lost in a maze of close to 100,000 km of blood vessels if a global tracking/navigation system similar to the Global Positioning System (GPS) for humans, is not provided. Therefore, when operating inside the vascular network, since imaging techniques relying on direct line-of-sight is not possible for servo-control purpose, gathering tracking information in order to guide such bacterial nanorobots to a specific targeted location inside the human body using the shortest or any desired paths without getting lost would require an appropriate imaging modality. Magnetic Resonance Imaging (MRI) systems already implemented in most clinics can be used for this purpose. This also adds further advantages especially during the planning phase where soft tissue and the blood vessels can be imaged in 3D.

As mentioned earlier, the magnetosomes embedded in the cell of each MC-1 magnetotactic bacterium are Fe_3O_4 single magnetic domain crystals of a few tens of nanometers in diameter and are used for directional control. Similarly, when placed inside the bore of a clinical scanner, these nanoparticles cause a local distortion of the high intensity DC magnetic field. Such local field distortion caused by each magnetosome can be estimated at a point P of coordinate r (x, y, z) by that of a magnetic dipole as

$$\vec{B}'(P) = \frac{\mu_0}{4\pi}\left(3\frac{(\vec{m}.\vec{r})\vec{r}}{r^5} - \frac{\vec{m}}{r^3}\right). \tag{17.1}$$

In (17.1), $\mu_0 = 4\pi 10^{-7}$ H m^{-1} represents the permeability of free space. The dipolar magnetic moment (A m^2) for a magnetosome uniformly magnetized by the high intensity of the MRI scanner is then given by

$$\vec{m} = \frac{4}{3}\pi a^3 \vec{M}_{SAT} \tag{17.2}$$

where the saturation magnetization of the magnetosome and its radius a (m) are taken into consideration. A numerical simulation of a single bacterium magnetic field perturbation plotted over an electron microscopy image assuming 11 aligned magnetosomes, each with a diameter of 70 nm has been plotted in Fig. 17.1. Since the homogeneity level of modern MRI clinical scanner is approximately 5 ppm over a 50 cm diameter spherical volume at 1.5 T, suggest that tracking of bacterial medical nanorobots inside the human body using existing medical imaging platforms is possible. This is confirmed experimentally in Fig. 17.4 where a swarm of MC-1 flagellated bacteria has been imaged with a 1.5 T clinical scanner.

In reality, because of the small overall size of each bacterial nanorobot, delivering sufficient therapeutic agents to a tumor would require more than one nanorobot. As such, directional control of a swarm or agglomeration of flagellated bacteria (or bacterial nanorobots since unlike other flagellated bacteria operating independently of computer commands, they represent fundamental self-propelled entities being controlled by computer in a closed-loop scheme) as shown in Fig. 17.4 will be essential in many instances. Using several bacteria simultaneously not only increases the amount of therapeutics being delivered but makes the tracking and hence the feedback control easier by increasing the signal intensity inside the human body. This is important since although the sensitivity of a clinical MRI system is very high, the limitation in the spatial resolution can be somewhat compensated for with a larger agglomeration of MTB. Furthermore, as depicted in Fig. 17.4, the percentage of bacteria in a specific region can also be evaluated with proper MRI sequences. This is important to evaluate the percentage of MTB that have reached the target. For delivering therapeutics to a tumor for example,

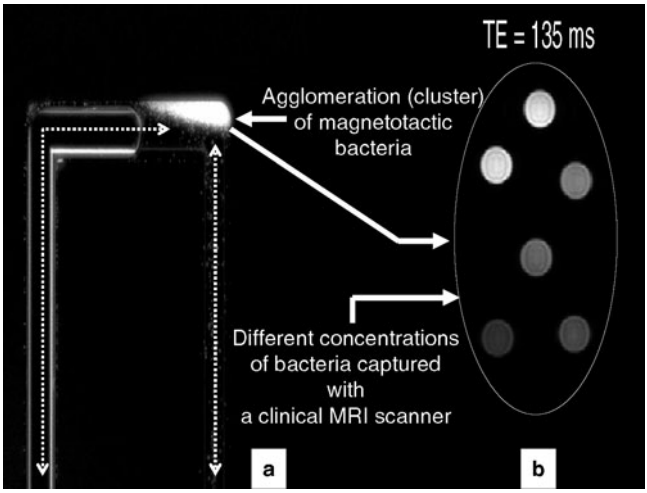

Fig. 17.4 (**a**) The figure shows an example of directional control of an agglomeration of MC-1 magnetotactic bacteria along the dotted path and (**b**), images taken with a clinical MRI system of various concentrations of MTB. The magnetosomes embedded in the cells affect the spin-spin (T2) relaxation times when imaged using fast spin echo sequence. (Images taken with a Siemens Avanto 1.5T clinical scanner using a wrist antenna with sequence parameters: TR/TE = 5,620/135 ms, slice thickness of 20 mm, and pixel spacing of 0.254 mm)

determining the percentage of bacterial nanorobots that has reached the target will indicate the amount of secondary toxicity delivered to the systemic blood circulatory system. In turn, this will indicate how many times the operations can be repeated without increasing secondary toxicity in the human body beyond a critical threshold. Similarly, if only one attempt is planned, this will indicate the maximum level of toxicity of the therapeutics that can be carried by the bacterial nanorobots for maximum efficacy at the tumoral lesion.

Figure 17.4a shows an agglomeration of MC-1 bacteria swimming in a tube mimicking a human blood vessel. Feedback directional control was done from tracking information gathered using an optical microscope (Fig. 17.4a). To the right in Fig. 17.4b, one can observe the intensity of the image from various concentration of MTB.

17.3 Envisioned Main Types of Medical Nanorobots

The human vasculature represents a complex environment where the variations in physiological properties represent new difficulties that must be dealt with. For instance, blood flow velocity in the arteries can reach one meter per second whereas

in the capillaries it can be as low as 1 mm/s. But in capillaries, because of the size of the blood cells, the medium cannot be considered homogeneous as in the arteries. Therefore, sending a nanorobot to a tumor could be somewhat similar to sending an exploration robot on the surface of planet Mars where different modules must be used to first escape the Earth gravitational force, then travel from the Earth to the orbit of Mars using closed-loop navigation control prior to use a landing module before releasing the exploration robot itself. Similarly, navigating from the release site in larger arteries at the catheterization limit to the tumoral region and passing through vessels such as the arterioles and capillaries, requires various types of microdevices/carriers and/or robots.

17.3.1 Bacterial Nanorobots

Bacterial nanorobots or nanorobots propelled by bacteria are most efficient in Low Reynolds conditions and particularly in the capillary networks. As mentioned earlier, unless designed to travel through the BBB, there is no apparent advantage to implement bacterial nanorobots designed to operate in the human microvasculature with an overall size of less than approximately 2 μm across. Actual designs of nanorobots capable of crossing the BBB are presently based on speculations without real development and experimental data and as such, it is not covered here due to a lack of experimental data and proof-of-concepts. Nonetheless, such devices capable of transiting through the BBB could indeed with the advancement in nanorobotics, become a potential topic in future publications.

The functionality of microscale nanorobots can be enhanced for operations in the human vasculature by taking advantage of the properties offered by nanometer-scale components. The propulsion system with the molecular motors and the flagella, the magnetosomes acting as tracking beacons and steering systems are just a few examples of that.

Because of their overall dimensions, engineers must think differently for the implementation of such microscale nanorobots compared to larger robots. For instance, several parts must rely on biochemistry instead of the more traditional mechanical approaches. As a simple example, a miniature mechanical gripper with recognition sensors for specificity in target recognition that may be connected to an onboard computer can be replaced with the integration of specific antibodies. Specific antibodies can also replace the glue or the screws used to assemble components in the implementation of larger robots. This is shown in Fig. 17.5 where a large bead emulating a potential artificial component is attached to a flagellated bacterium to build a hybrid microscale nanorobot. Other types of antibodies, bacteriophages, ligands, functionalized molecules, and peptides are only a few examples of components that can be used to emulate grippers, implement specificity or to embed target recognition, attach components, anchor the nanorobot, and/or to load therapeutic or other types of agents, to name but a few typical functions.

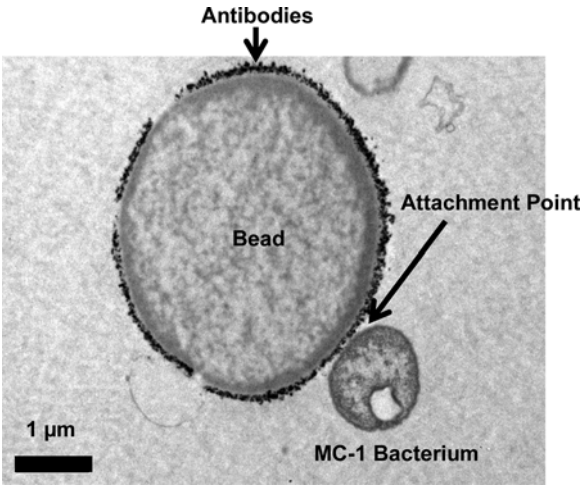

Fig. 17.5 One MC-1 flagellated bacterium being attached reliably to large bead emulating a potential artificial part of a hybrid nanorobot

For instance, loading the bacterial nanorobots can be done in many ways. For example, the MC-1 cell can be loaded with fluorescent cell penetrating peptide which could also be replaced by cytotoxic or radio-active agents. Nanometer-scale biodegradable polymeric nanoparticles loaded with cytotoxic or other agents can also be attached to the cell of the MC-1 bacterium using specific antibodies, again as depicted in the example in Fig. 17.5 where a relatively large artificial structure (here represented by a simple bead) which could be a synthetic part of an hybrid robot, has been attached to a bacterium using specific antibodies.

Bacterial nanorobots have huge advantages compared to an entirely synthetic version. For instance, MC-1-based bacterial nanorobots have superior performance in smaller diameter capillaries over synthetic counterparts such as ferromagnetic-based microrobots propelled by magnetic gradients when operating inside a relatively large animal or an adult size human body.

But the use of non-pathogenic MC-1 bacteria as propulsion system for micro-scale robots has some potential drawbacks that do not exist in synthetic versions. Indeed, initial tests conducted in human blood at 37°C showed that the velocity of the MTB and denoted v_{B37} at a time t (expressed in minutes and within the lifetime of approximately 40 min for the MC-1 bacterium when exposed to the environmental conditions of the human microvasculature) would decrease continuously according to (17.3).

$$v_{B37} = 0.09\, t^2 - 8.10\, t + v_{\mathrm{MTB}}. \tag{17.3}$$

In (17.3), v_{MTB} is the average velocity of the MTB (approximately 188 μm/s depending on cultivation parameters) prior to be exposed to the environmental conditions of the human microvasculature.

Even with such a decrease in velocity when exposed to environmental conditions inside the human body, flagellated MC-1 bacterial nanorobots would remain more effective for at least the time period required to target the tumoral lesion (estimated to be less than approximately 30 min although more tests are required to confirm it) when operating in the human body compared to a synthetic version such as a ferromagnetic microscale robot of similar size with force induced using continuous (50% duty cycle) 500 mT/m gradients being approximately the maximum gradients that can be applied at the human scale (e.g., to accommodate an adult size human torso) inside an upgraded MRI platform.

Effort could be done towards extending the operating life of the bacterium in the human microvasculature using approaches such as the ones relying on RNA. But the lifespan of such bacterium should remain short enough to prevent the bacteria to reproduce, becoming pathogens and a potential threat for the human body. On the other hand, the lifespan and the motility of these bacteria should be sufficient to allow them to reach their targets. Previous studies indicate that 40 min with previously recorded velocities of the MC-1 would most likely be sufficient for such task.

17.3.2 Synthetic Microscale Medical Robots and Carriers

Although bacterial nanorobots may have many advantages especially when we consider their very high efficiency for traveling in the microvasculature including larger capillaries, they become much less effective in larger diameter blood vessels where blood flow is much higher than the blood velocity levels found in the capillary networks. As a simple example to give an idea of their effectiveness, when in an arteriole having a diameter of 100 μm for instance, the bacterial nanorobots will have to deal with an expected average Poiseuille blood flow rate of approximately 0.52 m/s and be able to steer adequately considering an estimated 50 mm between successive blood vessel bifurcations. In this particular environment, an entirely synthetic ferromagnetic nanorobot of approximately 25 μm in diameter and loaded at 50%vol. with proven biocompatible Fe_3O_4 nanoparticles (which has a relatively low saturation magnetization of 0.5 compared to other options), will still perform better. In this case, this synthetic microscale robot will have a velocity of approximately 500 μm/s which is by far higher that the fastest bacterial nanorobot (initial maximum velocity of approximately 300 μm/s) under the same physiological conditions. Although recent experimental results show that the maximum velocity of the MC-1 bacteria can be increased beyond this value, several complementary types of medical nanorobots are still likely to be required considering the very high blood velocity in larger diameter vessels to allow targeting operations deeper in the microvasculature using bacterial nanorobots being carried near the targeting sites using synthetic micro-carriers. So far, recent results and proof-of-concepts suggest that such synthetic untethered micro-carriers and

robots will have embedded ferromagnetic or superparamagnetic materials to allow propulsion by magnetic gradients generated by an external source.

It is now known that a ferromagnetic core can be propelled, tracked, and controlled in real-time along a pre-planned path in blood vessels by using magnetic gradients applied in a 3D space. This was shown experimentally *in vivo* in the carotid artery of a living swine [15], an animal model close to human. Equation (17.4) explains the basic principle to induce a propulsion and steering force on ferromagnetic object.

$$\vec{F} = R \cdot V\left(\vec{M} \cdot \nabla\right) \vec{B}. \tag{17.4}$$

The force (17.4) induced on a ferromagnetic core with a volume V within an untethered micro-carriers or robots, depends in great part on the duty cycle R when the propulsion gradients are applied. This duty cycle is limited for two main reasons. First, propulsion cannot be executed when MRI is being performed since the magnetic propulsion gradients would interfere with the imaging gradients used for image slice selection in the bore of the MRI scanner. Second, in particular instances, the coils generating the propulsion gradients may overheat and when this is the case, the duty cycle must be decreased further to allow sufficient time for the coils to cool down to remain within an operational temperature range. All this will contribute to lower the efficiency of the propulsion method especially when the overall dimensions of the ferromagnetic robot become smaller.

Another factor to consider is the magnetization of the core material. Fortunately, when placed in the homogeneous DC magnetic field of 1.5 or 3 T found in modern scanners, it will reach the saturation level (M_{SAT}). Another factor affecting the propulsion force is the maximum gradient that can be applied. Initial estimations and designs suggest that the 40 mT/m of actual clinical MRI scanners could be increased to a maximum level of approximately 500 mT/m with a duty cycle of approximately 50% (to allow for tracking and/or cooling). Preliminary works suggest, although this remains a challenging engineering task at the present time, that this could be feasible within the space constraints inside the bore of a clinical MRI scanner while maintaining sufficient room to place an adult size human.

Nonetheless, since the induced force from magnetic gradients is proportional to the effective volume of magnetic material being embedded in the microscale nanorobot, a given synthetic microscale nanorobot would have to be as large as possible (i.e., with a diameter of approximately half the diameter of the blood vessels being traveled) to gather enough propulsion/steering force to cope with the blood flow in larger diameter vessels. But by doing so, such microscale nanorobot would not be able to transit from larger to smaller diameter blood vessels and will most likely create an undesired embolization.

An approach to resolve this issue is the use of an agglomeration of synthetic microscale robots or carriers. At such a scale and when placed in the high DC magnetic field of an MRI scanner, a magnetic dipole will develop for each microscale robots. This will create a dipole-dipole interaction or attraction force between each robot. The objective is to create a strong enough dipole-dipole interaction to

increase the effective volume of magnetic material to achieve a higher induced displacement force to cope with the higher flow rate while having a sufficiently low dipole-dipole interaction to allow such agglomeration to change shape when transiting from larger to narrower vessel diameters. Methods such as modifying the characteristics of the surface of each robot can be used to adjust such trade-off in dipole-dipole interaction.

17.4 Combining Synthetic and Bacterial Microscale Nanorobots to Reach Deeper Regions in the Human Vasculature

As stated earlier, preliminary data indicate that a combination of synthetic (artificial) and biological (bacterial) nanorobots would be required for tumor targeting. For instance, the data gathered using a synthetic version indicate that using 50%vol. to allow room for therapeutic loads of material having the highest magnetization saturation (M_{SAT}) of 2.45 T and an overall size equal to the cell of a single MC-1 bacterium required for operations and navigation in the smallest diameter capillaries under realistic conditions where a diameter of 4–5 μm is expected with 1 mm between bifurcations, and an average Poiseuille blood flow in the order of 0.5 mm/s, will be able to reach a maximum velocity of approximately 4 μm/s. At such velocity, it would be very difficult to operate/navigate within physiological conditions in the angiogenesis networks where the vasculature has narrowed diameter vessels and an impressive number of vessel bifurcations. Looking at one of the most advanced synthetic propulsion system in the form of an artificial flagella built from nanocoils [16] being propelled with the use of a rotating magnetic field where a velocity in a aqueous medium and without flow suggests that it would not be enough for such environment unless the blow flow is completely stopped or at least slowed down significantly. Indeed, the latter achieved a velocity of approximately 4.6 μm/s and as such, it cannot compete with the initial average velocity of approximately 200 μm/s (initial distribution between approximately 30–300 μm/s) of the MC-1 bacteria used as propulsion for the bacterial nanorobots. But as mentioned earlier, the same bacterial nanorobots would be useless in larger diameter vessels where the blood flow is much larger. As such, a combination of synthetic and bacterial nanorobots and/or carriers will be required for many targeting applications performed through the human vasculature. This is shown schematically in Fig. 17.6.

In Fig. 17.6, Large Embolization and Transport (LET) microscale carriers may take various forms. One preferred implementation consists of an entity that is made of several types of material depending on the applications and embedded functionalities required. Within such entity, magnetic nanoparticles are encapsulated with the therapeutic agents to be released if chemo-embolization is supported. For LET, an agglomeration of MTB is also encapsulated. The nanoparticles encapsulated in the polymeric shell can be Fe_3O_4 nanoparticles for proven biocompatibility

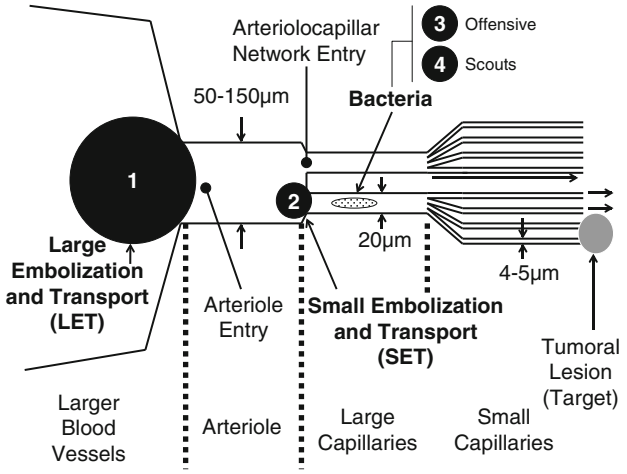

Fig. 17.6 Simple schematic showing the use of synthetic and bacterial microscale robots with their respective operating regions in the human vasculature for tumor targeting

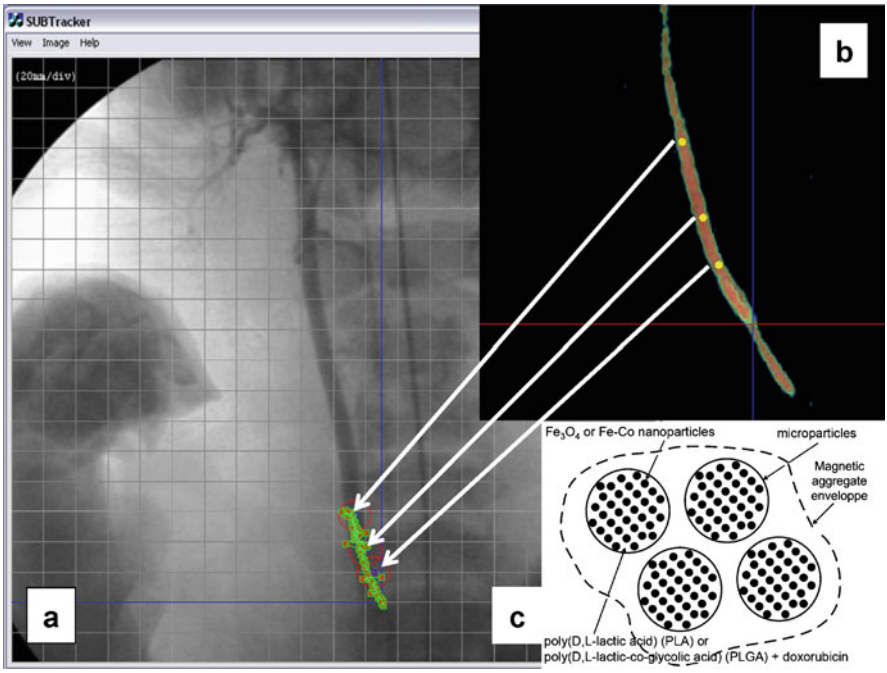

Fig. 17.7 Computer-controlled motion of a 1.5 mm ferromagnetic core in the artery of a living swine using 40 mT/m gradients generated by a clinical MRI scanner; (**a**) corresponding waypoints indicating the planned path being plotted on an acquired imaged of the artery; and (**b**) schematic representation of an agglomeration of magnetic carriers

but relatively low magnetization saturation or FeCo nanoparticles for enhanced propulsion/steering force density through a higher magnetization saturation level. In cases of FeCo, the nanoparticles are often designed to prevent toxic Cobalt ions to come in direct contact with blood. The number of nanoparticles is chosen high enough to provide an effective V for sufficient propulsion/steering force to be induced using magnetic gradients as described in (17.4). This is shown in Fig. 17.7a.

The magnetic nanoparticles are distributed throughout the inner structure to provide in addition to propulsion/steering, local magnetic field distortions (see 17.1) similar to MRI contrast agents that can be exploited for MR-tracking. The overall diameter of the nanoparticles is also chosen in many instances to allow hyperthermia-based computer-triggered release when other release methods such as the ones relying on a time-biodegradable polymer are not used.

Without upgrading typical clinical MRI scanner, the minimum size of each LET carrier is limited to approximately 250 μm across. This size is adequate for navigation in larger blood vessels using the 40 mT/m of each of the three orthogonal gradient coils already implemented in clinical MRI scanner for slice selection during MRI if a blood flow reduction technique such as the use of a balloon catheter is adopted. This will help since the pulsating flow rate in larger arteries may reach a peak velocity of approximately 1 m/s in human. An example of a relatively large ferromagnetic body being navigated in an artery of a living swine (an animal model relatively close to human) is depicted in Fig. 17.7a with the waypoints indicating the planned trajectory in the artery being depicted in Fig. 17.7b. The overall size of the LET carrier would prevent its entrance or navigation in smaller diameter vessels such as the arterioles since embolization would occur before getting deeper in the vasculature. As such, an agglomeration of LET entities (Fig. 17.7c) relying on a proper level of dipole-dipole interaction to aggregate would allow a large quantity of bacterial nanorobots to be transported simultaneously and beyond the entrance of the arterioles. Nonetheless, such LET carriers would create an embolization relatively far from the entrance of capillary network and hence would release such bacterial nanorobots further away from the tumor site. In such a case, the distance separating the tumor and the releasing site would become problematic and may decrease the targeting efficacy especially for targets located deeper in the microvasculature. In order to decrease the distance between the release (embolization) site and the tumor (target) site for instance, Small Embolization and Transport (SET) carriers can be used. The minimum size of each SET carriers would be approximately 40 μm across to create an embolization prior to be brought back to the systemic circulation. Furthermore, such size is also the limit (because of the effective volume of magnetic material that can be embedded) to apply effective steering force for navigation purpose using the highest magnetic gradient amplitude of approximately 500 mT/m that today's technology allows at the human scale (relative to an adult size torso) within the constraints of modern clinical scanners.

Indeed, if the hardware of the MRI scanner is upgraded to provide higher gradient amplitudes, then an agglomeration of SET entities or carriers can be

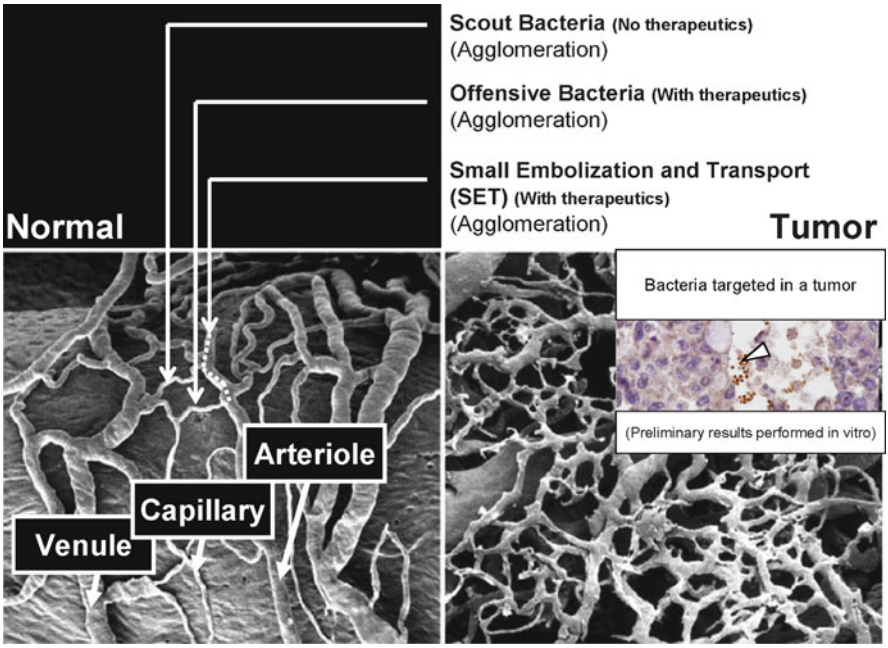

Fig. 17.8 Photographs of the various types of blood vessels with examples of locations accessible to the various types of entities (*left*) and a photograph showing the complexity of a tumoral angiogenesis network (*right*)

envisioned for releasing bacteria closer to the target at the arteriocapillar entry. The smaller number of bacterial nanorobots embedded per SET carriers can be compensated with a larger number of SET carriers. These flagellated bacteria or bacterial nanorobots could be scout bacteria or nanorobots, or offensive bacteria or nanorobots. This is depicted in Fig. 17.8.

Agglomerations of scout bacteria acting like controllable MRI contrast agents can be sent first in order to validate an appropriate path to the target. MRI sequences can be used to estimate the percentage of scout MTB that have reached the target provided that the population is sufficient for the sensitivity and spatial resolution of the scanner. Because of the initial higher risk of missing the target, these scouts unlike the offensive bacteria which transport toxic agents, have no therapeutic or toxic compounds and hence would avoid an increase of secondary toxicity in case they missed their target and reach the systemic circulation through the venules. Once a proper path is determined, offensive bacteria can then be used.

17.5 Conclusion

The complementary use of synthetic and hybrid nanorobots would typically yield better targeting when the target must be reached by navigating through the

microvasculature. Although flagellated MTB of type MC-1 with thrust exceeding 4 pN are more efficient when transiting though the capillary networks, they will prove to be useless in larger blood vessels in normal conditions. Therefore, synthetic carriers such as the ones made of polymeric and ferromagnetic materials have been proposed for the transport of these bacteria through the larger blood vessels and towards the release sites at the arteriocapillar network entry if a reduction of the blood flow using instruments such as balloon catheters is not applicable. The displacement behavior of MTB can also be taken into account to avoid the need for traditional feedback control since existing medical imaging modalities do not have a sufficiently high spatial resolution to image small blood vessels such as capillaries. Hence, bacterial nanorobots defined here in its most basic form as MTB navigating under computer control have the capability to enhance targeting in complex microvasculature. Other types of medical nanorobots with different capabilities are under development and were not presented here to maintain the chapter at an introductory level. Indeed, in this chapter, only the fundamental types have been briefly presented as an introduction in this new field of research that may offer promising avenues for the next generation of medical interventions.

References

1. Drexler, K.E.: Nanosystems: molecular machinery, manufacturing, and computation, John Wiley and Sons, New York (1992)
2. Martel, S.: Method and system for controlling micro-objects or micro-particles, U.S. Pat. Appl. 11/145,007 (2005)
3. Martel, S.: Targeted delivery of therapeutic agents with controlled bacterial carriers in the human blood vessels. In: 2nd ASM/IEEE EMBS Conference on Bio, Micro and Nanosystems. San Francisco, USA, 2006
4. Darnton, N., Turner, L., Breuer, K., Berg, H.C.: Moving fluid with bacterial carpet. Biophys. J. **86**, 1863–1870 (2004)
5. Behkam, B., Sitti, M.: Bacterial flagella-based propulsion and on/off motion control of microscale objects. Appl. Phys. Lett. **90**, 023902–023904 (2007)
6. Steager, E., Kim, C-B., Patel, J., Bith, S., Naik, C., Reber, L., Kim, M.J.: Control of microfabricated structures powered by flagellated bacteria using phototaxis. Appl. Phys. Lett. **90**, 263901–263903 (2007)
7. Martel, S.: Controlled bacterial micro-actuation. In: Proceedings of International Conference on Microtechnology in Medicine and Biology (MMB), Okinawa, Japan, 2006
8. Martel, S., Tremblay, C., Ngakeng, S., Langlois, G.: Controlled manipulation and actuation of micro-objects with magnetotactic bacteria. Appl. Phys. Lett. **89**, 233804–233806 (2006)
9. Berg, H.C., Brown, D.A.: "Chemotaxis in Escherichia coli analyzed by three-dimensional tracking. Nature. **239**, 500–504 (1972)
10. Ford, R.M., Phillips, B.R., Quinn, J.A., Lauffenburger, D.A.: Measurement of bacterial random motility and chemotaxis coefficients. I. Stopped-flow diffusion chamber assay. Biotech. Bioeng. **37**(7), 647–660 (1991)
11. Armitage, J.P.: Bacterial motility and chemotaxis. Sci. Prog. **76**, 451–477 (1992)
12. Frankel, R.B. Blakemore, R.P.: Navigational compass in magnetic bacteria. J. Magn. Magn. Mater. **15–18**(3), 1562–1564 (1980)

13. Denham, C., Blakemore, R., Frankel, R.: Bulk magnetic properties of magnetotactic bacteria. IEEE Trans. Magnetism. **16**(5), 1006–1007 (1980)
14. Debarros, H., Esquivel, D.M.S., Farina, M.: Magnetotaxis. Sci. Prog. **74**, 347–359 (1990)
15. Martel, S., Mathieu, J-B., Felfoul, O., Chanu, A., Aboussouan, É., Tamaz, S., Pouponneau, P., Beaudoin, G., Soulez, G., Yahia, L'H., Mankiewicz, M.: Automatic navigation of an untethered device in the artery of a living animal using a conventional clinical magnetic resonance imaging system. Appl. Phys. Lett. **90**(11), 114105–114107 (2007)
16. Bell, D.J., Leutenegger, S., Hammar, K.M., Dong, L.X., Nelson, B.J.: Flagella-like propulsion for microrobots using a nanocoil and a rotating electromagnetic field. In: Proceedings of the IEEE International Conference on Robotics and Automation (ICRA), pp. 1128–1133 (2007)